

TECHNICAL ADVANCE/RESOURCE

Deployment of the *Burkholderia glumae* type III secretion system as an efficient tool for translocating pathogen effectors to monocot cells

Shailendra Sharma¹, Shiveta Sharma¹, Akiko Hirabuchi¹, Kentaro Yoshida^{1,2}, Koki Fujisaki¹, Akiko Ito¹, Aiko Uemura¹, Ryohei Terauchi¹, Sophien Kamoun², Kee Hoon Sohn^{2,†}, Jonathan D. G. Jones² and Hiromasa Saitoh^{1,*}

¹Iwate Biotechnology Research Center, Kitakami, Iwate, 024-0003, Japan, and

²The Sainsbury Laboratory, John Innes Centre, Norwich Research Park, Norwich, NR4 7UH, UK

Received 21 January 2013; revised 01 February 2013; accepted 7 February 2013; published online 2 March 2013.

*For correspondence (e-mail saitoh@ibrc.or.jp).

†Present address: Institute of Agriculture and Environment, Massey University, Private Bag 11222, Palmerston North, 4442, New Zealand.

SUMMARY

Genome sequences of plant fungal pathogens have enabled the identification of effectors that cooperatively modulate the cellular environment for successful fungal growth and suppress host defense. Identification and characterization of novel effector proteins are crucial for understanding pathogen virulence and host-plant defense mechanisms. Previous reports indicate that the *Pseudomonas syringae* pv. *tomato* DC3000 type III secretion system (T3SS) can be used to study how non-bacterial effectors manipulate dicot plant cell function using the effector detector vector (pEDV) system. Here we report a pEDV-based effector delivery system in which the T3SS of *Burkholderia glumae*, an emerging rice pathogen, is used to translocate the AVR-Pik and AVR-Pii effectors of the fungal pathogen *Magnaporthe oryzae* to rice cytoplasm. The translocated AVR-Pik and AVR-Pii showed avirulence activity when tested in rice cultivars containing the cognate *R* genes. AVR-Pik reduced and delayed the hypersensitive response triggered by *B. glumae* in the non-host plant *Nicotiana benthamiana*, indicative of an immunosuppressive virulence activity. AVR proteins fused with fluorescent protein and nuclear localization signal were delivered by *B. glumae* T3SS and observed in the nuclei of infected cells in rice, wheat, barley and *N. benthamiana*. Our bacterial T3SS-enabled eukaryotic effector delivery and subcellular localization assays provide a useful method for identifying and studying effector functions in monocot plants.

Keywords: pEDV system, *Magnaporthe oryzae*, mCherry, nuclear localization signal, confocal microscopy, hypersensitive response, technical advance.

INTRODUCTION

Pathogens secrete a battery of proteins called effectors that help the invasion of host plants (Hann *et al.*, 2010; Koeck *et al.*, 2011; Stassen and Van den Ackerveken, 2011). Pathogen-associated molecular patterns (PAMPs) are recognized by plants via pattern recognition receptor proteins and activate PAMP-triggered immunity (PTI; Boller and He, 2009; Zipfel, 2009). Successful pathogens secrete effector proteins and target host cellular components to suppress PTI. On the contrary, effector-triggered immunity (ETI) is manifested after recognition of one or more effectors by corresponding host disease resistance (*R*) proteins. Effector-triggered immunity often involves gene for gene relationships culminating in the hypersensitive response (HR),

which is generally triggered by the interaction between plant *R* gene products and pathogen effectors called avirulence (AVR) proteins (Jones and Dangl, 2006; van der Hoorn and Kamoun, 2008; Thomma *et al.*, 2011).

Plant pathogenic fungi cause important yield losses in crops. Identification of new fungal effectors and their functions is crucial for a better understanding of the virulence of fungal pathogens and host-plant defense capabilities. Fungal pathogens probably secrete their effectors from invasive hyphae or haustoria. Apoplastic and cytoplasmic effectors are the two major categories of effectors based on the host target sites (Kamoun, 2006; Mueller *et al.*, 2008; Mosquera *et al.*, 2009; Khang *et al.*, 2010). Cytoplasmic

effector proteins have been inferred from either their localization inside the host cell or their recognition by host cytoplasmic R proteins. The recent availability of genome sequence information of many diverse fungal pathogens has enabled the identification of various secreted effector proteins (Yoshida *et al.*, 2009; Fabro *et al.*, 2011; Bozkurt *et al.*, 2012). However, the following steps, such as functional analysis of candidate effector proteins, often involve time-consuming and laborious procedures (e.g. generation of stable transgenic plants). Sometimes it is also difficult to genetically manipulate the fungal pathogens for candidate effector genes, making the whole process of effector functional analysis laborious and cumbersome.

Translocation of effector proteins to host cells using the type III secretion system (T3SS) of bacterial pathogens provides a fast alternative to the above-mentioned approaches. In plant systems, a calmodulin-dependent adenylate cyclase assay involving accumulation of cyclic AMP has been widely used to demonstrate the T3SS-dependent translocation of the *Xanthomonas* effector protein AvrBs2 in pepper (Casper-Lindley *et al.*, 2002), the *Pseudomonas syringae* effector protein AvrPto in tomato and the *Nicotiana benthamiana* (Schechter *et al.*, 2004) and *Erwinia amylovora* effector protein DspA/E in tobacco (Triplett *et al.*, 2009). Furthermore, the utilization of bacterial T3SS to translocate and study functions of oomycete effector proteins has been recently shown in several studies (Sohn *et al.*, 2007; Whisson *et al.*, 2007; Rentel *et al.*, 2008; Fabro *et al.*, 2011). The T3SS of the bacterial potato pathogen, *Pectobacterium atrosepticum* was utilized to see intracellular recognition of *Phytophthora infestans* (the potato late blight disease pathogen) effector AVR3a *in planta*. Secretion of AVR3a as a fusion protein by the T3SS was demonstrated by co-infiltration of *N. benthamiana* leaves with *Agrobacterium tumefaciens* that delivered the R gene *R3a*, and yielded a clear HR (Whisson *et al.*, 2007). In the other studies, authors employed the T3SS of *P. syringae* to translocate downy mildew *Hyaloperonospora arabidopsidis* (*Hpa*; formerly *Hyaloperonospora parasitica*) effectors into host *Arabidopsis thaliana* (Arabidopsis) and non-host turnip plants. The *Hpa* effectors ATR1 and ATR13 can be delivered from *P. syringae* by replacing the signal peptide and RxLR motif that are necessary for secretion in oomycete pathogens with the N-terminus of the bacterial effectors AvrRps4 or AvrRpm1 (Sohn *et al.*, 2007; Rentel *et al.*, 2008). This technique has enabled the study of *Hpa* cytoplasmic effectors by monitoring *in planta* growth of *P. syringae* delivering virulent or avirulent variants of ATR1 and ATR13 into susceptible or resistant Arabidopsis accessions. The effector detector vector (pEDV) system utilizes the N-terminal portion of AvrRps4 that is necessary and sufficient for T3SS-dependent delivery and *in planta* processing. The pEDV system was further used for screening candidate effectors predicted in the genome sequence of the *Hpa* isolate

Emoy2, investigating suppression of host Arabidopsis and non-host turnip defenses (Fabro *et al.*, 2011). However, to date the pEDV system has not been applied to deliver pathogen effectors into monocots.

In the present study, we set out to develop an efficient and robust eukaryotic effector delivery system in monocot plants. We demonstrate the use of the pEDV system to deploy the T3SS of the bacterial pathogen *Burkholderia glumae* to translocate effector proteins into monocot plant cells. *Burkholderia glumae* causes grain rot, seedling rot and panicle blight in rice and bacterial wilt in many field crops. This bacterium has been reported from major rice growing regions around the world and is now considered as an emerging major pathogen of rice (Tsushima *et al.*, 1996; Jeong *et al.*, 2003; Kim *et al.*, 2010; Ham *et al.*, 2011).

The ascomycete fungus *Magnaporthe oryzae* causes the devastating fungal disease of rice known as blast (Zeigler *et al.*, 1994; Couch and Kohn, 2002; Talbot, 2003). Owing to its high economic importance, it is highly desirable to identify new *M. oryzae* effectors to further decipher their function in order to develop an effective disease control strategy. We first apply the *B. glumae* (BG)-pEDV system to understand the *Magnaporthe*-rice pathosystem (Valent, 1990; Saitoh *et al.*, 2012). We demonstrate the translocation and avirulence function of two *M. oryzae* AVR effector proteins, namely AVR-Pii and AVR-Pik (Yoshida *et al.*, 2009), using the BG-pEDV system in rice plants. Next, we show that the BG-pEDV effector delivery assay is not only suitable for rice but also for a dicot species, *Nicotiana benthamiana*, and other monocot species, *Triticum aestivum* and *Hordeum vulgare*, that have been recalcitrant to systematic effector delivery experiments.

RESULTS

Intracellular localization of fluorescent effector proteins in rice

Previously we cloned two avirulence (AVR) genes, AVR-Pik and AVR-Pii from *M. oryzae* (Yoshida *et al.*, 2009). Since both AVRs seem to be recognized by nucleotide binding site-leucine rich repeat (NB-LRR) type R-proteins that are presumably localized in rice cell cytoplasm, we hypothesized that the subcellular localization of AVR-Pik and AVR-Pii effectors is also in rice cell cytoplasm. In order to confirm the translocation of AVR-Pik and AVR-Pii from *M. oryzae* to rice cell cytoplasm, we fused AVR-Pik and AVR-Pii with the reporter protein mCherry and modified a small nuclear localization signal (NLS) from simian virus large T-antigen (Kosugi *et al.*, 2008). This fusion of the NLS to the fluorescent effectors facilitates the intracellular visualization of translocated effectors, as reported in recent studies (Khang *et al.*, 2010; Saitoh *et al.*, 2012). Khang *et al.* (2010) also reported that secreted fluorescent effectors preferentially accumulate in biotrophic interfacial complexes (BICs) at the invasive

hyphae–rice cell interface. We inoculated leaf sheaths of a susceptible rice cultivar Shin-2 with *M. oryzae* isolate Sasa2 expressing *AVR-Pik:mCherry:NLS* or *AVR-Pii:mCherry:NLS* transgenes. Thirty hours after inoculation, we performed confocal laser-scanning microscopy analysis (confocal microscopy) of infected leaf sheaths. mCherry fluorescent signals were observed in BICs and the nuclei of leaf sheath cells infected with *M. oryzae* transformants expressing AVR:mCherry:NLS, suggesting translocations of the fusion proteins into rice cell cytoplasm through invasive fungal hyphae (Figure 1a, upper panels). To exclude the possibility that the NLS led the translocation of the proteins, we inoculated *M. oryzae* isolate Sasa2 expressing *AVR-Pik:mCherry* (+*AVR-Pikp:Ak:mCherry*) or *AVR-Pii:mCherry* (+*AVR-Piip:Ai:mCherry*) into rice cultivar Shin-2 leaf sheaths. AVR:mCherry fusion proteins were also observed in the nuclei of rice cells (Figure 1a, lower panels) but showed lower frequencies than that the proteins with NLS.

Additionally, to demonstrate whether the mCherry fusions of the two AVRs retain Avr function, we inoculated

+*AVR-Pikp:Ak:mCherry* and +*AVR-Piip:Ai:mCherry* into rice plants harboring *Pik* and *Pii* *R*-genes, respectively. We used the wild-type (WT) strain (Sasa2 WT that lacks *AVR-Pik* and *AVR-Pii*) as a negative control, and a transformant harboring an intact copy of *AVR-Pik* (+*AVR-Pikp:AVR-Pik*) and a transformant harboring an intact copy of *AVR-Pii* (+*AVR-Piip:AVR-Pii*) as positive controls. The rice cultivars Kanto 51 (harboring *Pik*) and Kakehashi (harboring *Pii*) were used to study incompatible interaction for AVR-Pik and AVR-Pii, respectively (Yoshida *et al.*, 2009). A rice cultivar, Moukoto, that lacks both *Pik* and *Pii* *R* genes was used to study compatible interactions for both effectors. In contrast to the Sasa2 WT, +*AVR-Pikp:AVR-Pik* and +*AVR-Pikp:Ak:mCherry* failed to cause disease in the rice cultivar Kanto51 (*Pik*⁺), and +*AVR-Piip:AVR-Pii* as well as +*AVR-Piip:Ai:mCherry* failed to infect the rice cultivar Kakehashi (*Pii*⁺; Figure S1a). Sasa2 WT and all the transformants successfully infected the rice cultivar Moukoto (*Pik*⁻, *Pii*⁻; Figure S1a), suggesting that the observed incompatibility in infected cultivars Kanto51 and Kakehashi was caused by *R*-AVR interactions.

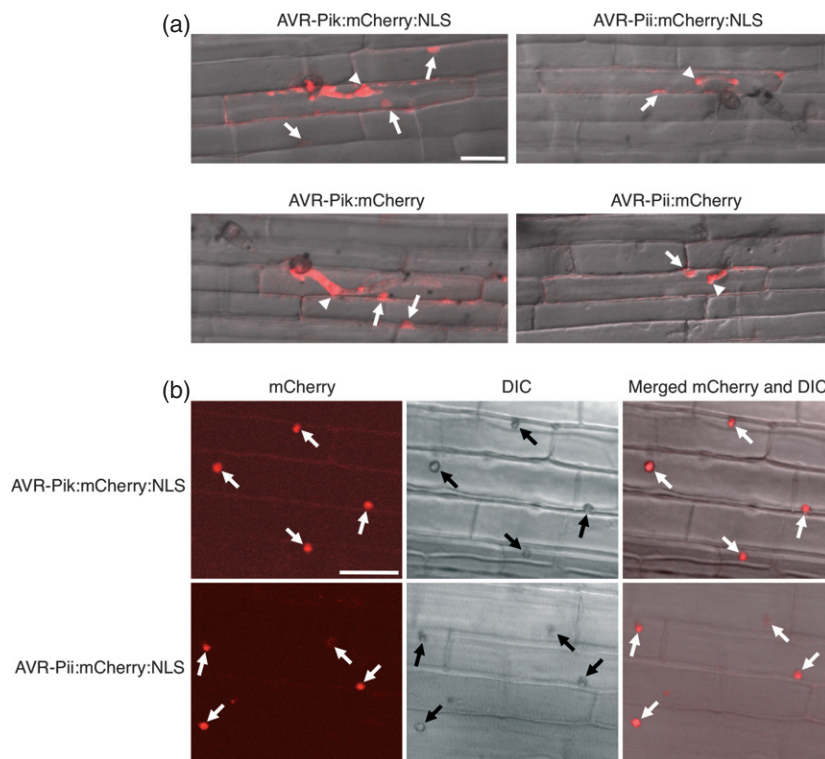


Figure 1. Fluorescently labeled AVR-Pik and AVR-Pii of *Magnaporthe oryzae* were localized in rice cytoplasm after secretion from invasive fungal hyphae as well as by *Burkholderia glumae* (BG) type III secretion system (T3SS).

(a) Localization of the fusion proteins in the nuclei of rice cultivar Shin-2 after infection with *M. oryzae* transformants expressing *AVR-Pik:mCherry:NLS* and *AVR-Pii:mCherry:NLS*, *AVR-Pik:mCherry* and *AVR-Pii:mCherry*. These fusion protein genes were expressed under the native promoters of *AVR-Pik* and *AVR-Pii*, respectively. Confocal laser-scanning microscopy analysis (confocal microscopy) was conducted 30 h post-inoculation. Each panel shows merged differential interference contrast (DIC) and mCherry (red) images. White arrows and arrowheads indicate mCherry fluorescence in the nuclei and biotrophic interfacial complexes (BICs), respectively. Scale bar is 20 μm.

(b) Localization of the fusion proteins AVR-Pik:mCherry:NLS and AVR-Pii:mCherry:NLS in the nuclei of rice cultivar Shin-2 after infection with BG-pEDV-AVR-Pik-mCN and BG-pEDV-AVR-Pii-mCN, respectively (pEDV, effector detector vector). Confocal microscopy was conducted 2 days post-inoculation. Left panels show mCherry images. Middle panels show the corresponding DIC images. Right panels show the merged mCherry and DIC images. White arrows in mCherry and merged images indicate fluorescence in the nuclei. Black arrows in the DIC image of leaf sheaths show the nuclei. Scale bar is 20 μm.

Active transcription of *AVR-Pik*, *AVR-Pik:mCherry*, *AVR-Pii* and *AVR-Pii:mCherry* genes in the transformants was confirmed by RT-PCR (Figure S1b). These results demonstrate that mCherry fusion proteins of AVR-Pik and AVR-Pii retain Avr function.

In order to test whether the two fusion proteins AVR-Pik:mCherry:NLS and AVR-Pii:mCherry:NLS can be translocated to rice cells by the *B. glumae* T3SS using the pEDV, we transformed *B. glumae* strain 106619 with the above transgenes *AVR-Pik:mCherry:NLS* and *AVR-Pii:mCherry:NLS* cloned in pEDV. These bacterial transformants, named BG-pEDV-AVR-Pik-mCN and BG-pEDV-AVR-Pii-mCN, were used for effector delivery in rice cells. Leaf sheaths of the rice cultivar Shin-2 were infiltrated with BG-pEDV-AVR-Pik-mCN and BG-pEDV-AVR-Pii-mCN, and after 2 days the epidermal cells were observed by confocal microscopy. The mCherry fluorescent signals were detected in the nuclei (Figure 1b). Although our attempt to stain the nuclei with 4',6-diamidino-2-phenylindole (DAPI) failed, presumably due to inefficient absorbance of the DAPI staining solution in living rice leaf sheath, shapes of nuclei could be clearly seen in the differential interference contrast (DIC) images (Figure 1b). Confocal microscopy of non-inoculated and BG-pEDV (harboring empty pEDV vector)-inoculated leaf sheaths did not show any mCherry fluorescence signals (Figure S2). These results suggest that the *B. glumae*-pEDV system supported translocation of the *M. oryzae* effector proteins into the rice cell cytoplasm similar to the native delivery system by *M. oryzae*.

Rice leaf sheath inoculation assay of *B. glumae* to monitor effector avirulence activity

After confirming translocation of effector proteins into rice cytoplasm, a leaf sheath inoculation assay was conducted to test the effector avirulence or virulence activity inside rice plant cells. First we checked the expression of effector proteins in *B. glumae*. The pEDV system utilizes AvrRps4N (1–137 amino acids of AvrRps4) that are sufficient for T3SS delivery and *in planta* processing. *Burkholderia glumae* transformed with three pEDV constructs harboring AvrRps4N:HA (termed BG-pEDV), AvrRps4N:HA:AVR-Pik (BG-pEDV-AVR-Pik) and AvrRps4N:HA:AVR-Pii (BG-pEDV-AVR-Pii) were cultured in Kings B broth. Western blot analysis of total bacterial protein extracts with anti-hemagglutinin (HA) antibody showed expression of AVR effector fusion proteins in the pEDV system (Figure 2a).

To confirm whether HA fusions to the N-termini of mature proteins (i.e. proteins without signal peptides) of rice blast AVRs are recognized when delivered from transgenic *M. oryzae*, we performed transformation of *M. oryzae* isolate Sasa2 with a construct *AVR-Pikp:signal peptide(sp):HA:AVR-Pik* and a construct *AVR-Piip:sp:HA:AVR-Pii*. We carried out rice inoculation assay with these two transformants *+AVR-Pikp:sp:HA:AVR-Pik*, *+AVR-Piip:*

sp:HA:AVR-Pii, as well as two positive control strains *+AVR-Pikp:AVR-Pik*, *+AVR-Piip:AVR-Pii*, and the wild-type strain (Sasa2 WT) as negative control. The rice cultivar Kanto51 harboring *Pik* inoculated with *+AVR-Pikp:AVR-Pik* and *+AVR-Pikp:sp:HA:AVR-Pik*, as well as the cultivar Kakehashi harboring *Pii* inoculated with *+AVR-Piip:AVR-Pii* and *+AVR-Piip:sp:HA:AVR-Pii* showed a resistance phenotype, whereas these two cultivars showed susceptibility when inoculated with Sasa2 WT (Figure S3a). All five strains successfully infected the susceptible rice cultivar Moukoto (*Pik*⁻, *Pii*⁻; Figure S3a) indicating that the resistance phenotype found in rice cultivars Kanto51 (*Pik*⁺) and Kakehashi (*Pii*⁺) was caused by AVR-R interactions. Active transcription of *AVR-Pik*, *HA:AVR-Pik*, *AVR-Pii* and *HA:AVR-Pii* genes in the transformants was confirmed by RT-PCR (Figure S3b). These results indicate that N-terminal HA fusions of the two AVRs retained Avr function.

To test whether HA fusion proteins of rice blast AVRs are recognized when delivered by *B. glumae*, rice leaf sheaths were injected with BG-pEDV-AVR-Pik, BG-pEDV-AVR-Pii or BG-pEDV. Bacterial growth patterns were monitored in both compatible and incompatible interactions 3 h (3 HPI) and 3 days (3 DPI) post-inoculation. We counted and compared the number of bacteria recovered from the inoculated plants. We measured the number of bacteria recovered from five independently inoculated leaf sheaths for each AVR-R combination. When leaf sheath of rice cultivar Kanto51 (*Pik*⁺) was inoculated with BG-pEDV-AVR-Pik and BG-pEDV, the number of recovered bacteria at 3 DPI was significantly lower for BG-pEDV-AVR-Pik than for BG-pEDV (Figure 3b). On the other hand, when rice cultivar Moukoto (*Pik*⁻) was infected with the same bacterial strains, there was no significant difference in growth between the two strains. For the interaction between AVR-Pii and *Pii*, we obtained similar results: growth of BG-pEDV-AVR-Pii bacteria was significantly lower than that of BG-pEDV on the rice cultivar Kakehashi (*Pii*⁺), whereas these two strains showed similar levels of growth on Moukoto (*Pii*⁻; Figure 3c).

To see whether a gene-for-gene specific HR was induced when AVR protein was delivered into rice, we performed rice leaf sheath injections with high doses of bacteria and looked for a microscopic indicator of HR-like cell death (dead cells stained with trypan blue) 3 DPI. However, we could not see significant differences in trypan blue stain between the AVR- and empty-vector harboring bacteria in both AVR-Pik and AVR-Pii tests.

Suppression of *B. glumae*-induced hypersensitive response by AVR-Pik in non-host plant *Nicotiana benthamiana*

Since a previous study reported that the wild-type *B. glumae* strain BGR1 elicits a strong HR in *N. tabacum* (Kang et al., 2008), we injected *B. glumae* strain 106619

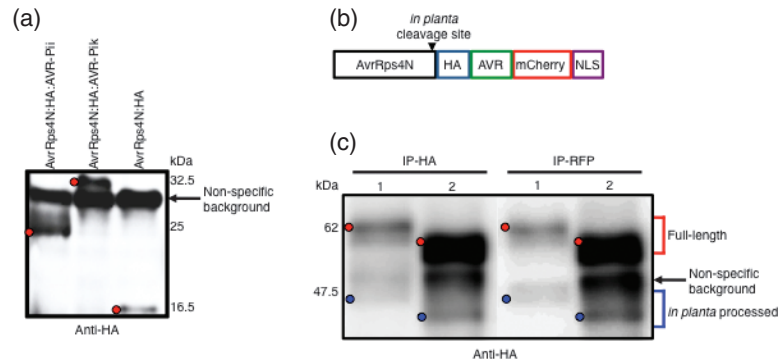


Figure 2. Expression of AvrRps4N:HA:AVR-Pii, AvrRps4N:HA:AVR-Pik, and expression and processing of AVR-Pik:HA:mCherry:NLS, AVR-Pii:HA:mCherry:NLS fusion proteins in the *Burkholderia glumae* (BG) type III secretion system (BG-T3SS).

(a) Western blot analysis of the hemagglutinin (HA)-tagged effector fusion proteins in *B. glumae* using anti-HA antibody.

(b) Schematic diagram of AvrRps4N:HA:AVR:mCherry:NLS chimeric protein which is expressed in BG-pEDV-AVR-Pik-mCN and BG-pEDV-AVR-Pii-mCN (pEDV, effector detector vector).

(c) Three-week-old *Nicotiana benthamiana* leaves were infiltrated with BG-pEDV-AVR-Pik-mCN (lane 1) and BG-pEDV-AVR-Pii-mCN (lane 2; $OD_{600} = 2.0$). Leaves were harvested 10 h post-infiltration and immunoprecipitation (IP) was performed using anti-HA and anti-red fluorescent protein (RFP) agarose beads. Immunoprecipitated proteins were used for Western blot analysis using anti-HA antibody. Bands corresponding to the full-length proteins are indicated by red dots, and those for processed proteins with expected sizes are indicated by blue dots.

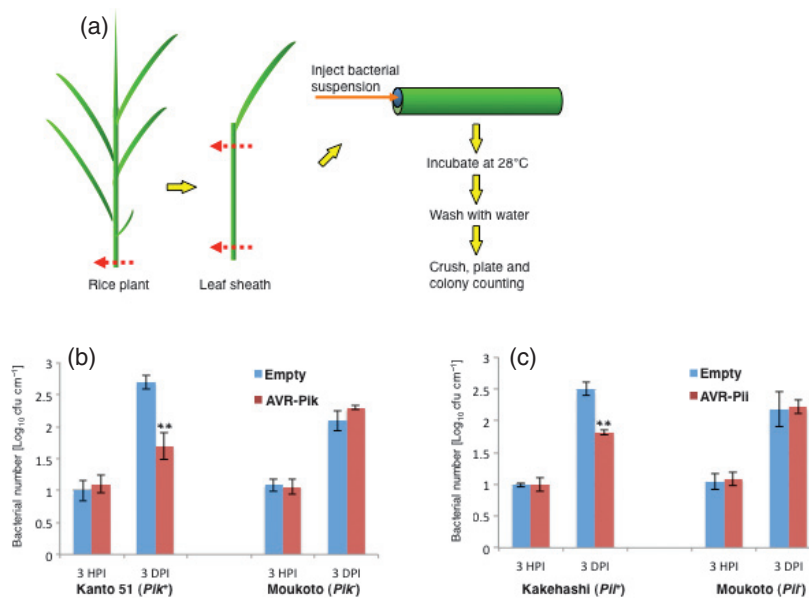


Figure 3. AVR-Pik and AVR-Pii delivered by the *Burkholderia glumae* (BG) type III secretion system (T3SS) reduced *B. glumae* growth in the rice cultivars harboring corresponding *R* genes.

(a) A cartoon depicting inoculation of rice leaf sheath with BG-pEDV-AVR-Pik or BG-pEDV-AVR-Pii and BG-pEDV (pEDV, effector detector vector).

(b) Bacterial growth in leaf sheath of rice plants infected with BG-pEDV-AVR-Pik and BG-pEDV (Empty).

(c) Bacterial growth in leaf sheath of rice plants infected with BG-pEDV-AVR-Pii and BG-pEDV. The number of bacterial cells was counted 3 h post-inoculation (HPI) and 3 days post-inoculation (DPI). Each bar represents the mean number of bacterial colonies recovered on gentamycin containing Kings B agar plates from five replicates. The standard error of the numbers is shown on each bar. Double asterisks represent a significant difference in bacterial colony numbers ($P < 0.01$) between the empty vector- and AVR transgene-harboring bacterial strains. These sets of experiments were repeated five times with similar results.

into *N. tabacum* and *N. benthamiana*, and observed a HR that was slower in *N. benthamiana* compared with in *N. tabacum*. Therefore, we decided to use *N. benthamiana* to see the cell death suppression effect of fungal effectors on non-host HR. In *N. benthamiana*, the onset of HR was observed around 36–45 HPI with small patches of desiccated tissue that became clearly visible around 55–58 HPI.

Clear tissue collapse was observed after 60 HPI. To observe the intracellular localization of mCherry-tagged effector proteins in *N. benthamiana*, we infiltrated BG-pEDV-AVR-Pik-mCN and BG-pEDV-AVR-Pii-mCN to *N. benthamiana* leaves. After 18 h of infiltration, we performed confocal microscopy on infiltrated leaf sections to detect fluorescent mCherry signals. Fluorescent mCherry signals were

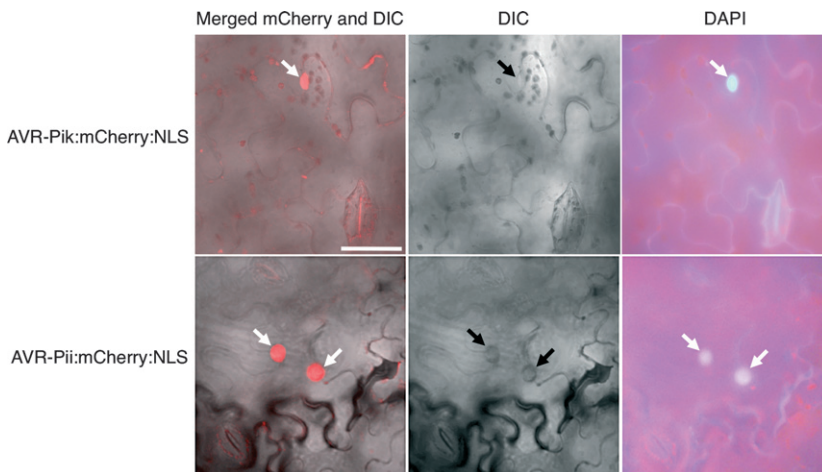


Figure 4. The *Burkholderia glumae* (BG) effector detector vector (pEDV) system targets fluorescently labeled AVR-Pik and AVR-Pii to *Nicotiana benthamiana* cytoplasm.

Localization of the fusion proteins AVR-Pik:mCherry:NLS and AVR-Pii:mCherry:NLS in the nuclei of *N. benthamiana* cells. The left panels show merged mCherry (red) and differential interference contrast (DIC) images. The middle panels show the DIC images. The right panels show 4',6-diamidino-2-phenylindole (DAPI) stained images. White arrows indicate mCherry fluorescence in the nuclei (left panels) and DAPI stained nuclei (right panels). Black arrows indicate in DIC images (middle panels) show the nuclei. Scale bar is 50 μ m.

observed in the nuclei for both cases (Figure 4). To confirm that fluorescent mCherry signals co-localized to the nuclei, we stained the infected leaf sections with DAPI. Localization of fluorescent mCherry signals corresponded to DAPI signals, confirming that both fusion proteins were delivered to *N. benthamiana* cell cytoplasm and accumulated in the nuclei (Figure 4). These results confirmed that T3SS of *B. glumae* could translocate the effector proteins to the inside of *N. benthamiana* cells.

To test whether delivery of the fluorescent protein fusions from *B. glumae* correlates with the delivery of processed tagged effector proteins to plant cells, total proteins were extracted from BG-pEDV-AVR-Pik-mCN- or BG-pEDV-AVR-Pii-mCN-infected *N. benthamiana* leaves. The extracts were immunoprecipitated (IP-ed) using anti-HA or anti-red fluorescent protein (RFP; that recognizes mCherry) agarose beads, the IP-ed proteins were separated by SDS-PAGE gel and the blots were probed with anti-HA antibody. Because the chimeric fusion proteins contain both HA and mCherry tags so that both full-length and *in planta* processed fusion proteins are expected to be detected after immunoprecipitation with anti-HA or anti-RFP antibody (Figure 2b). Western blot analysis revealed the presence of full-length fusion proteins AvrRps4N:HA:AVR-Pik:mCherry:NLS, AvrRps4N:HA:AVR-Pii:mCherry:NLS and *in planta* processed HA:AVR-Pik:mCherry:NLS, HA:AVR-Pii:mCherry:NLS at 10 HPI in *N. benthamiana* leaves (Figure 2c). These results demonstrate that AvrRps4N signal could properly deliver both N- and C-terminally tagged effector proteins to plant cells, and that the AvrRps4N signal peptide was properly processed upon delivery. Sohn *et al.* (2007) showed that an *in planta* processed form of the *Hyaloperonospora arabidopsidis* effector ATR13 fusion protein AvrRps4N:ATR13:HA expressed in *P. syringae* pv. *tomato* (*Pst*) appeared at a much lower level than the non-processing form made in bacteria in the strain-infected *A. thaliana* leaves. The detection ratio between the full-length and *in planta* processed form of AvrRps4N:ATR13:HA in the above research

is comparable to that of AvrRps4N:HA:AVR:mCherry:NLS fusion protein expressed in *B. glumae* in the BG-pEDV-AVR-mCN-infected *N. benthamiana* in the present study (Figure 2c). These results indicate that the pEDV system in *Pst* and *B. glumae* can be used similarly to deliver effector proteins into plant cells.

To investigate the effect of AVR-Pik and AVR-Pii on *B. glumae*-induced non-host HR, inocula of BG-pEDV-AVR-Pik, BG-pEDV-AVR-Pii and BG-pEDV (Empty) were suspended in 0.9% w/v NaCl ($OD_{600} = 0.75$) and infiltrated into *N. benthamiana* leaves. Interestingly, BG-pEDV-AVR-Pik triggered a considerably reduced and delayed HR in comparison to BG-pEDV that triggered a strong HR (Figure 5a; upper panels). In contrast, infiltration of BG-pEDV-AVR-Pii caused HR comparable to BG-pEDV (Figure 5a, middle panels). NaCl (0.9% w/v) did not induce any visible symptoms (Figure 5a, lower panels). To check the growth of the bacteria harboring different constructs, bacterial numbers in the leaves were recorded 0, 1, 2 and 3 DPI. There was no significant difference in bacterial numbers between BG-pEDV-AVR-Pik and BG-pEDV (Figure 5b) and between BG-pEDV-AVR-Pii and BG-pEDV (Figure 5c) at the four time points. This result indicates that the reduced HR in BG-pEDV-AVR-Pik was not caused by the reduction of bacterial numbers in this treatment.

Translocation of effector proteins into wheat and barley cells

To test the possibility of effector translocation by the BG-pEDV system in monocot species other than rice, we used young leaf sheaths and cut leaves of wheat and barley for inoculation. Leaf sheaths were examined by confocal microscopy at 3 DPI similar to rice. In addition, cut leaves were also examined at 3 DPI by confocal microscopy without peeling the epidermis. Fluorescent mCherry signals were detected in the nuclei of both leaf sheath and cut leaf cells of wheat and barley (Figure 6). Although DAPI staining of the nuclei of living cells of wheat and barley

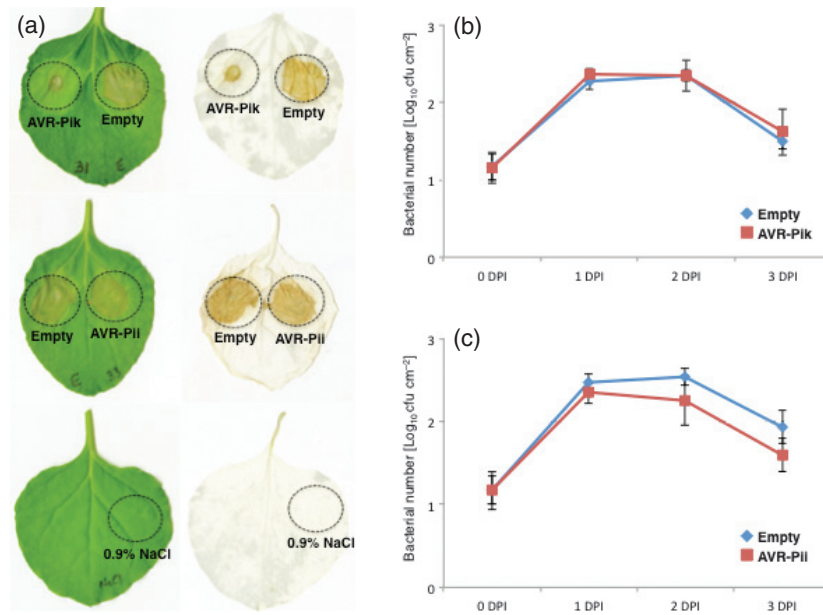


Figure 5. AVR-Pik suppressed non-host hypersensitive response (HR) induced by *Burkholderia glumae* (BG) in *Nicotiana benthamiana*.

(a) *Nicotiana benthamiana* leaves were infiltrated with BG-pEDV-AVR-Pik (uppermost panels) and BG-pEDV-AVR-Pii (middle panels; pEDV, effector detector vector). The opposite area of each leaf was also infiltrated with BG-pEDV (Empty). Leaf area infiltrated with bacterial inocula is shown by dashed circle. As a negative control, *N. benthamiana* leaf was infiltrated with 0.9% w/v NaCl (lowest panels). Right panels show ethanol treated leaves to enhance visibility of the HR cell death. Photographs were taken 5 days post-inoculation (DPI).

(b), (c) Bacterial numbers of *N. benthamiana* leaves infiltrated with (b) BG-pEDV-AVR-Pik and BG-pEDV, and (c) BG-pEDV-AVR-Pii and BG-pEDV. Bacterial numbers were counted 0, 1, 2 and 3 DPI. The line graph represents the mean number of bacterial numbers recovered at the four time points. Standard deviations are shown for each time point. This experiment was repeated three times with similar results.

failed, shapes of the nuclei could be seen clearly in the DIC images of leaf sheath cells, similar to rice. For cut leaf cells, the presence of thick cuticle on the epidermis of wheat and barley made the visualization of the shape of the nuclei difficult in the DIC images (Figure 6). In summary, live-cell imaging suggested that fluorescently labeled effectors were translocated to wheat and barley cells, similar to rice.

DISCUSSION

Previous studies demonstrated that oomycete effectors can be delivered via the T3SS of *Pst* using the pEDV on dicot plants (Sohn *et al.*, 2007; Fabro *et al.*, 2011). These studies suggested the possibility of utilization of the pEDV system for other bacteria pathogenic to monocot plants.

A Gram-negative bacterium *B. glumae* (formerly *Pseudomonas glumae*) causes panicle blight, grain rot, sheath rot and seedling rot in rice (Tsushima *et al.*, 1996; Ham *et al.*, 2011). Therefore, we selected *B. glumae* for employing a pEDV system to see the function of fungal effectors in the host rice cells. Generally, inoculation at seedling stage (using a syringe or spraying method) is used for *B. glumae* pathology experiments dealing with sheath rot or panicle blight, respectively (Nandakumar *et al.*, 2009). However, to visualize effector delivery and measure bacterial growth properly *in planta*, we employed a rice leaf sheath inoculation assay at the seedling stage like rice–blast interactions (Saitoh *et al.*, 2012). The results in the

present study proved that effectors translocated through T3SS of *B. glumae* into the rice cytoplasm and maintain their functional role, and hence prove the utility of the pEDV system for studying the function of effectors in rice.

The elicitation of a strong HR after *B. glumae* infection on *Nicotiana benthamiana* provided us with an opportunity to test the effector activity (virulence) in non-host plants. A comparatively reduced and delayed HR was observed after the inoculation of BG-pEDV-AVR-Pik in comparison to inoculation of BG-pEDV indicating the suppression of non-host disease resistance by AVR-Pik and hence its possible virulence activity in non-host plants (Figure 5a). However, there is a possibility that AVR-Pik induced unexpected plant defense responses as an elicitor, and reduced bacterial growth resulting in the attenuated cell death. Therefore, we compared the growth of BG-pEDV-AVR-Pik and BG-pEDV bacterial strains in *N. benthamiana* leaves. The results showed that bacterial growth was the same between the two strains (Figure 5b), indicating that the effect of AVR-Pik on suppressing cell death is caused by its virulence function rather than elicitor activity.

In previous studies using the *Pst*-pEDV system to investigate virulence function of alleles of *Hpa* effector ATR13 and other effector candidates that suppress PTI leading to increased bacterial growth, authors employed a Δ CEL (conserved effector locus) mutant strain of *Pst* which is unable to suppress PAMP-triggered cell wall defense (cal-

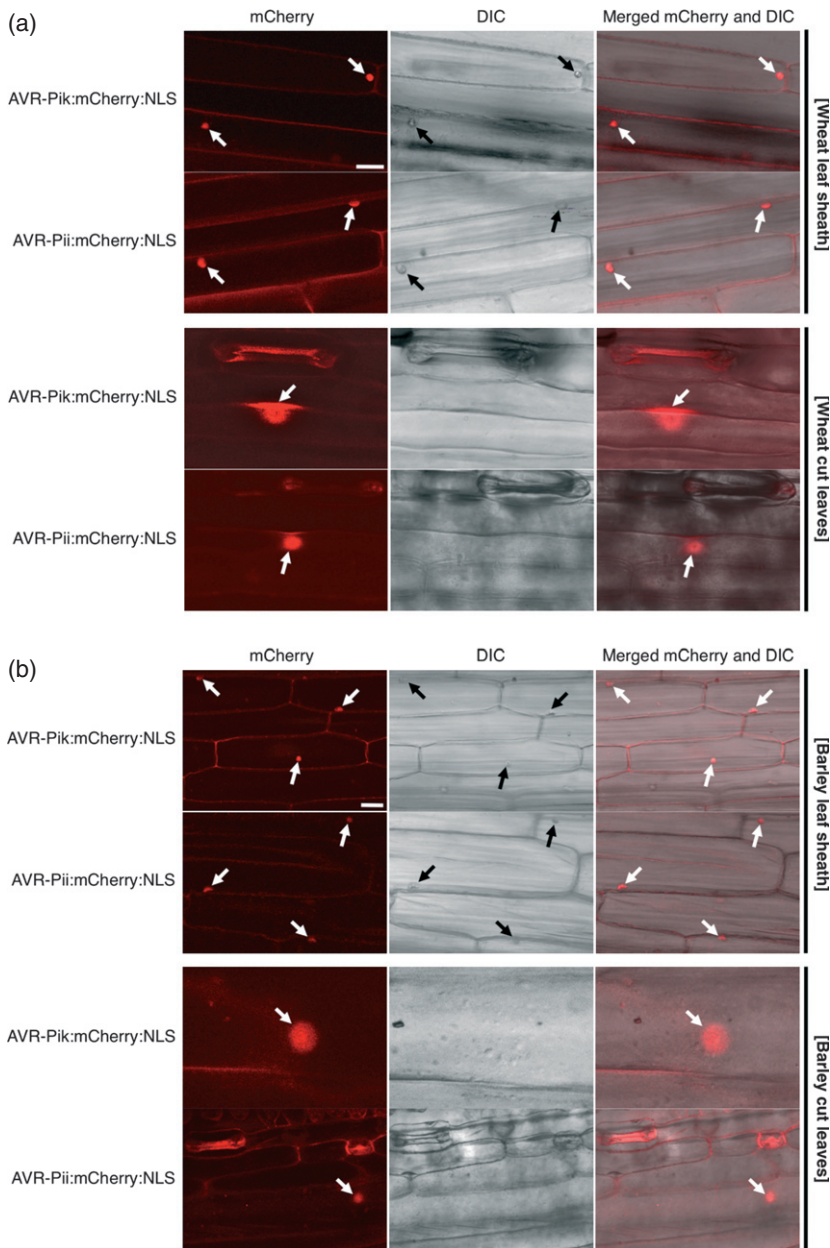


Figure 6. Fluorescently labeled AVR-Pik and AVR-Pii were localized in wheat and barley cytoplasm using the *Burkholderia glumae* (BG) effector detector vector (pEDV) system.

Localization of the fusion proteins AVR-Pik:mCherry:NLS and AVR-Pii:mCherry:NLS in the nuclei of wheat (a) and barley (b) leaf sheath and cut leaf cells. Left panels show mCherry images. Middle panels show the differential interference contrast (DIC) images. Right panels show the merged mCherry and DIC images. White arrows in mCherry and merged images indicate fluorescence in the nuclei. Black arrows in DIC images of leaf sheaths indicate the nuclei. The nuclei were not observed in the DIC images of cut leaf cells presumably due to the presence of thick cuticle on the epidermis. Scale bars are 20 μm .

lose deposition; Sohn *et al.*, 2007; Fabro *et al.*, 2011 [‘arabidopsis (*Hpa*) effector’ was replaced by ‘*Hpa* effector’ on 08.05.2013 after original online publication]). The CEL contains at least four characterized effector genes involved in suppression of PTI so that *Pst*- Δ CEL can no longer suppress callose deposition (Debroy *et al.*, 2004). The reason why they used *Pst*- Δ CEL for analyzing the virulence function of *Hpa* effectors is to avoid masking the virulence function of *Hpa* effectors by pre-existing *Pst* DC3000 effectors located on the CEL that confer suppression of PTI. In the present study, no significant differences in bacterial growth were detected in the susceptible rice cultivar Moukoto lacking *Pik* and *Pii* after BG-pEDV-AVR-Pik or BG-pEDV-AVR-Pii inoculation in comparison to BG-pEDV inoculation

(Figure 3b,c). However, there is a possibility that the virulence activity of AVR-Pik or AVR-Pii is masked by pre-existing effector activity of *B. glumae*.

For wheat and barley, we checked symptoms in intact living plants after stem inoculation with *B. glumae* but clear sheath rot phenotype was not observed. Nevertheless, fluorescently tagged effectors are clearly detected in the cytoplasm of wheat and barley cells via T3SS of *B. glumae*. Therefore, our BG-pEDV system provides a new opportunity to utilize genome sequencing information to identify and characterize novel cytoplasmic effector proteins of economically important pathogens in monocots. Translocation and localization of *M. oryzae* effectors to rice as well as wheat and barley demonstrated that the

BG-pEDV system is suitable for effector discovery from important pathogens of cereal crops, including cereal-infecting rust and powdery mildew fungi. Future technical improvement may allow us to identify secreted proteins from wheat and barley eukaryotic pathogens with virulence or Avr function at the BG-pEDV-effector inoculation sites. We foresee that further analysis will reveal other applications of the BG-pEDV system in monocots.

EXPERIMENTAL PROCEDURES

Plasmid construction

A 0.3-kb AVR-Pik cDNA fragment was amplified from the plasmid pCB1004-*pe*x31-D (Yoshida *et al.*, 2009) with the primers Xba1_*kozak_**pe*x31_U1 (5'-GCTCTAGAAAAGTCAATATGCGTGTACCACTT-3'; the XbaI site is underlined) and BamHI-AVRPikwoStop-R (5'-CTGGATCCGAAGCCGGCCCTTTTTTCCCAA-3'; the BamHI site is underlined). The PCR product was digested with XbaI and BamHI, and introduced into pCB-Ppw12-mCherry-NLS (Saitoh *et al.*, 2012) to produce pCB-Ppw12-AVR-Pik-mCherry-NLS. A 1.4-kb AVR-Pik promoter fragment (AVR-Pikp) was amplified from the plasmid pCB1004-*pe*x31-D (Yoshida *et al.*, 2009) with the primers NotI-*pe*x31-U1 (5'-ATAAGAAATGCGGCGCAAAGGAATAAGCGGACC-3'; the NotI site is underlined) and Xba1-AVRPik-pro-R (5'-GCTCTAGACAAAATAATGTCTTTTGCAAACAAAG-3'; the XbaI site is underlined). The PCR product was digested with NotI and XbaI, and Ppw12 in pCB-Ppw12-AVR-Pik-mCherry-NLS was replaced with AVR-Pikp to produce pCB-AVR-Pikp-AVR-Pik-mCherry-NLS.

A 0.8-kb DNA fragment containing AVR-Pii promoter and coding regions (AVR-Piip-AVR-Pii) was amplified from the plasmid pCB1531-*pe*x33 (Yoshida *et al.*, 2009) with the primers M13 RV (5'-CAGGAAACGCTATGAC-3') and KF159r (5'-AATCGGATCCGTTGCATTTA TGATTTAAATACGC-3'; the BamHI site is underlined). The PCR product was digested with NotI and BamHI, and pCB-AVR-Pikp-AVR-Pik-mCherry-NLS (described above) was replaced with AVR-Piip-AVR-Pii to produce pCB-AVR-Piip-AVR-Pii-mCherry-NLS.

An mCherry fragment was prepared by digestion of pCB-Ppw12-mCherry-stop (Saitoh *et al.*, 2012) by XhoI and EcoRI, and mCherry-NLS in pCB-AVR-Pikp-AVR-Pik-mCherry-NLS was replaced with mCherry to produce pCB-AVR-Pikp-AVR-Pik-mCherry. An mCherry fragment was prepared by digestion of pCB-Ppw12-mCherry-stop by BamHI and EcoRI, and mCherry-NLS in pCB-AVR-Piip-AVR-Pii-mCherry-NLS was replaced with mCherry to produce pCB-AVR-Piip-AVR-Pii-mCherry.

A 1.1-kb fragment of AVR-Pik-mCherry-NLS without a signal peptide was amplified with the primers XP31nsU2 (5'-CCGCTCGAGGAAACGGGCAACAAATATATAG-3'; the XhoI site is underlined) and FNL1 (5'-GCCTGATCATTAAAGCTCCATAATCTACCTTTCC-3'; the FbaI site is underlined) using pCB-AVR-Pikp-AVR-Pik-mCherry-NLS as a template. The PCR product was digested with FbaI and digested partially with XhoI for 5 min, and a 1.1-kb fragment was then introduced into Sall and BamHI sites of pEDV5 (Fabro *et al.*, 2011), generating pEDV-AVR-Pik-mCN. A 1.0-kb fragment of AVR-Pii-mCherry-NLS without signal peptide was amplified with the primers XP33nsU2 (5'-CCGCTCGAGCTTCCCACTCCGGCCAGCCTG-3'; the XhoI site is underlined) and FNL1 using pCB-AVR-Piip-AVR-Pii-mCherry-NLS as a template. The PCR product was digested with FbaI and digested partially with XhoI for 5 min, and a 1.0-kb fragment was then introduced into Sall and BamHI sites of pEDV5, generating pEDV-AVR-Pii-mCN. A 0.3-kb fragment of AVR-Pik without signal peptide (AVR-Pikns) was

amplified with the primers nP31S (5'-ACGCGTTCGACGAACGGGCAACAAATATAT-3'; the Sall site is underlined) and P31RB (5'-CGGGATCCAAAGCCGGGCTTTTTTC-3'; the BamHI site is underlined) using pCB-AVR-Pikp-AVR-Pik-mCherry-NLS as a template. The PCR product was digested with Sall and BamHI, and introduced into the same sites of pEDV5, generating pEDV-AVR-Pik. A 0.2-kb fragment of AVR-Pii without a signal peptide (AVR-Piins) was amplified with the primers nP33S (5'-ACGCGTTCGACCTTCCCACTCCGGCCAGCCT-3'; the Sall site is underlined) and P33RB (5'-CGGGATCCGTTGCATTTATGA TAAAATACG-3'; the BamHI site is underlined) using pCB-AVR-Piip-AVR-Pii-mCherry-NLS as a template. The PCR product was digested with Sall and BamHI, and introduced into the same sites of pEDV5, generating pEDV-AVR-Pii.

A 1.6-kb fragment of AVR-Pikp-sp (signal peptide) was amplified from pCB1004-*pe*x31-D with the primers M13 RV and XP31spL1 (5'-GCTCTAGAGGCATTGACGACAGCGACAG-3'; the XbaI site is underlined). The PCR product was digested with NotI and XbaI, and Ppw12 in pCB-Ppw12-mCherry-NLS was replaced with AVR-Pikp-sp to produce pCB-AVR-Pikp-sp-mCherry-NLS. A 0.3-kb fragment of HA-AVR-Pikns was amplified with the primers XHAU1 (5'-GCTCTAGAGTCTATCCGTACGACGTACC-3'; the XbaI site is underlined) and EP31L1 (5'-GGAATTCTTAAAAGCCGG GCCTTTTTTCCCC-3'; the EcoRI site is underlined) using pEDV-AVR-Pik as a template. The PCR product was digested with XbaI and EcoRI, and mCherry-NLS in pCB-AVR-Pikp-sp-mCherry-NLS was replaced with HA-AVR-Pikns to produce pCB-AVR-Pikp-sp-HA-AVR-Pikns. A 0.6-kb fragment of AVR-Piip-sp was amplified from pCB1531-*pe*x33 with the primers M13 RV and XP33spL1 (5'-GCTCTAGATGCTGCGATTCCGATTGCATATAATGC-3'; the XbaI site is underlined). The PCR product was digested with NotI and XbaI, and Ppw12 in pCB-Ppw12-mCherry-NLS was replaced with AVR-Piip-sp to produce pCB-AVR-Piip-sp-mCherry-NLS. A 0.2-kb fragment of HA-AVR-Piins was amplified with the primers XHAU1 and EP33L1 (5'-GGAATTCTTAGTTGCATTTATGATTTAAAATACGCG-3'; the EcoRI site is underlined) using pEDV-AVR-Pii as a template. The PCR product was digested with XbaI and EcoRI, and mCherry-NLS in pCB-AVR-Piip-sp-mCherry-NLS was replaced with HA-AVR-Piins to produce pCB-AVR-Piip-sp-HA-AVR-Piins.

Fungal strain, medium and transformation

The *M. oryzae* strain Sasa2 used in this study is stored at the Iwate Biotechnology Research Center (Yoshida *et al.*, 2009). To obtain protoplasts, hyphae of *M. oryzae* strains were incubated for 3 days in 200 ml of YG medium (0.5% yeast extract and 2% of glucose, w/v). Protoplast preparation and transformation were performed as described previously (Takano *et al.*, 2001). Bialaphos-resistant transformants were selected on plates with 250 µg ml⁻¹ of bialaphos (Wako Pure Chemicals, <http://www.wako-chem.co.jp/english/>). A wild-type strain Sasa2 was transformed with pCB-AVR-Pikp-AVR-Pik-mCherry-NLS, pCB-AVR-Piip-AVR-Pii-mCherry-NLS, pCB-AVR-Pikp-AVR-Pik-mCherry, pCB-AVR-Piip-AVR-Pii-mCherry, pCB-AVR-Pikp-sp-HA-AVR-Pikns and pCB-AVR-Piip-sp-HA-AVR-Piins.

Rice blast pathogenicity assay

Fungal inocula were prepared as described in Saitoh *et al.* (2012). Rice leaf inoculation was performed as follows: conidial suspension (5 × 10⁵ conidia ml⁻¹) containing Tween 20 (0.01% in final concentration) was sprayed onto rice seedlings (cultivars Kanto 51, Kakehashi or Moukoto) of the fourth leaf stage. Inoculated plants were placed in a

dew chamber at 27°C for 24 h in the dark, and then transferred to the growth chamber with a photoperiod of 16 h. Rice cultivar Kanto 51 (containing the *Pik R* gene) and Kakehashi (containing the *Pii R* gene) were used for studying incompatible interaction and a cultivar without *Pik* or *Pii R* genes, namely Moukoto, was used for the studying compatible interaction.

***Burkholderia glumae* competent cells preparation and transformation**

Burkholderia glumae strain 106619 was obtained from NIAS (National Institute of Agrobiological Sciences) Genebank, Tsukuba, Ibaraki, Japan. Glycerol stock of the wild-type strain was prepared and stored at –80°C. For preparing competent cells of the wild-type strain, 10 µl of glycerol stock was inoculated to 20 ml of LB medium in a 50-ml tube and further incubated at 28°C for 16–40 h with horizontal shaking until OD₆₀₀ = 0.8 was achieved. The lid of the tube was opened for 30 sec under a clean bench. The tube was incubated again at 28°C for 4 h with horizontal shaking. Thereafter, the tube was centrifuged twice at 800 *g* at 4°C for 5 min. Each time the pellet was dissolved in 20 ml of autoclaved cold 10% glycerol. Finally the pellet was dissolved in 200 µl of cold 10% glycerol and divided into 50-µl aliquots and stored at –80°C for a further transformation step.

Each construct was transformed to *B. glumae* using electroporation (Bio-Rad Gene Pulser Xcell®, <http://www.bio-rad.com/>). Transformed strains were plated on a Kings B agar plate containing 25 p.p.m. gentamycin. At least four glycerol stocks were prepared for each transformant and stored at –80°C. *Burkholderia glumae* transformed with empty pEDV5 (Fabro *et al.*, 2011), pEDV-AVR-Pik, pEDV-AVR-Pii, pEDV-AVR-Pik-mCherry-NLS and pEDV-AVR-Pii-mCherry-NLS are called hereafter BG-pEDV, BG-pEDV-AVR-Pik, BG-pEDV-AVR-Pii, BG-pEDV-AVR-Pik-mCN and BG-pEDV-AVR-Pii-mCN, respectively. These bacterial transformants were stored at –80°C for further use.

Expression of HA-tagged AVR effectors in *B. glumae* and Western blotting

Low-salt LB medium was inoculated with BG-pEDV-AVR-Pik, BG-pEDV-AVR-Pii and BG-pEDV and incubated at 28°C for 60 h with vigorous horizontal shaking of 150 strokes per min. After adjusting to OD₆₀₀ = 0.9, cultures were centrifuged at 3300 *g* for 3 min. Pellets were resuspended in autoclaved *hypersensitive response and pathogenicity* (*hrp*)-inducing media (Fabro *et al.*, 2011) and again incubated at 28°C for 15 h with vigorous horizontal shaking. Cultures were again centrifuged at 3300 *g* for 3 min. Pellets were resuspended in cold protein extraction buffer [Protease inhibitor cocktail (Sigma, <http://www.sigmaaldrich.com/>); 2 µl in 1 ml extraction buffer], 20 mM TRIS (2-amino-2-(hydroxymethyl)-1,3-propanediol) HCl (pH 7.5), 1 mM EDTA (pH 8.0), 5 mM DTT, 150 mM NaCl, 1% Triton X-100, 0.1% SDS, 10% glycerol] and vortexed properly. Vortexed suspensions were further sonicated and centrifuged at 18 000 *g* for 5 min. at 4°C. Chilled acetone (2.5 × volume) was added to supernatants and vortexed gently. The acetone-concentrated protein solutions were stored at –20°C for a minimum of 2 h. This was followed by centrifugation at 18 000 *g* for 5 min at 4°C. Pellets were dissolved in autoclaved distilled water. To completely dissolve the pellets, Eppendorf tubes were rubbed with a rough surface. After completely dissolving the pellets, these crude extracts were either stored at –20°C or further used for SDS PAGE and Western blotting. The crude extracts (15 µl per lane) were sep-

arated on a 10–20% pre-cast e-PAGE (ATTO, <http://www.attotech.com/>) and the proteins were transferred onto Immobilon Transfer Membranes (Millipore, <http://www.millipore.com/>). The blots were blocked in 2% ECL Advance Blocking Agent (GE Healthcare, <http://www.gehealthcare.com/>) in TTBS (10 mM TRIS-HCl (pH 7.5), 100 mM NaCl, 0.1% Tween 20) for 1 h at 23°C with gentle agitation. For immunodetection, blots were probed with anti-HA (3F10)-HRP (Roche, <http://www.roche.com/>) in a 1:10 000 dilution in TTBS for 2 h. After washing the membrane for 10 min three times, the reactions were detected using an ECL Advance Western blotting detection reagents (GE Healthcare) and a Luminescent Image Analyzer LAS-4000 (Fujifilm, <http://www.fujifilm.com/>).

Preparation of bacterial inoculum

For rice and *N. benthamiana* pathogenicity tests, frozen glycerol stocks of BG-pEDV, BG-pEDV-AVR-Pik and BG-pEDV-AVR-Pii were streaked on Petri plates with Kings B agar medium containing 25 p.p.m. gentamycin. These Petri plates were incubated at 28°C. After 2 days of incubation bacterial colonies were suspended in autoclaved distilled water for rice and in 0.9% w/v NaCl for *N. benthamiana* pathogenicity tests. Optical density (OD₆₀₀) was fixed for each experiment. For effector localization experiments, inocula of BG-pEDV-AVR-Pik-mCN and BG-pEDV-AVR-Pii-mCN were prepared in the same way.

Rice leaf sheath inoculation assay

Forty- to 50-day-old leaf sheaths were inoculated with BG-pEDV-AVR-Pik, BG-pEDV-AVR-Pii or BG-pEDV inocula (OD₆₀₀ = 0.5). Inoculated leaf sheaths were placed at 28°C under moist conditions in plastic plates. Three hours post-inoculation and 3 DPI, leaf sheaths were properly washed with autoclaved distilled water from the inner side using a 1-ml syringe with a 26-µm gauge needle. Washed leaf sheaths were ground in pestle and mortar in 10 mM MgCl₂. This slurry was further serially diluted a thousand times in 10 mM MgCl₂ and finally 10 µl of diluted slurry was plated on Kings B medium containing 25 p.p.m. gentamycin. Petri plates were incubated at 28°C, and colony counting was then performed (Figure 3a).

***Nicotiana benthamiana* pathogenicity test**

Leaves of 3-week-old *N. benthamiana* plants were infiltrated with bacterial inocula of OD₆₀₀ = 0.75 using a 1-ml syringe without a needle. A half section of leaf was injected with BG-pEDV-AVR-Pik or BG-pEDV-AVR-Pii and the other half section was injected with BG-pEDV. Plants were kept at 23°C. Timing of the HR was recorded thereafter. To observe the HR more clearly, we followed the decolorization protocol with a slight modification described earlier (Tomita *et al.*, 2011).

For recording bacterial counts, bacterial inocula of OD₆₀₀ = 0.45 were injected to *N. benthamiana* leaves. Leaf disk samples of diameter 5 mm were collected using a cork borer at 0, 1, 2 and 3 DPI. Leaves of three separate plants, as three replicates, were used for collecting samples. From each leaf sample, three leaf disks were collected at a given time point. Leaf disks were ground in cold 10 mM MgCl₂ and processed further as described above for the rice leaf sheath inoculation assay.

Intracellular effector localization and microscopy analysis

For effector localization in rice using *M. oryzae*, a wild-type strain Sasa2 was transformed with pCB-AVR-Pikp-AVR-Pik-mCherry-NLS and pCB-AVR-Piip-AVR-Pii-mCherry-NLS. Fungal inocula were prepared as described in Saitoh *et al.* (2012). Conidial suspension

(1×10^5 conidia ml⁻¹) was inoculated into the leaf sheath of rice cultivar Shin-2 and Sasanishiki. These inoculated leaf sheaths were placed at 25°C under moist and dark conditions in plastic plates. After 30 h, these leaf sheaths were subjected to confocal laser-scanning microscopy analysis (confocal microscopy).

For effector localization in rice using *B. glumae*, bacterial inoculum (OD₆₀₀ = 0.75) of BG-pEDV-AVR-Pik-mCN or BG-pEDV-AVR-Pii-mCN were inoculated in 35 to 45-day-old leaf sheaths of rice cultivar Shin-2. These inoculated leaf sheaths were placed at 28°C under moist and dark conditions in plastic plates. After 2 days, these leaf sheaths were subjected to confocal microscopy. Both young leaf sheaths and cut leaves were used for effector localization experiments in wheat (cultivar Nebarigoshi) and barley (cultivar Nigrate). Leaf sheaths were immersed in bacterial inoculum (OD₆₀₀ = 0.75) of BG-pEDV-AVR-Pik-mCN and BG-pEDV-AVR-Pii-mCN and incubated at 27°C. Confocal microscopy was performed, on the third day after inoculation, after washing the leaf sheaths with distilled water. Cut leaves were immersed in bacterial inoculum (OD₆₀₀ = 0.75) of BG-pEDV-AVR-Pik-mCN and BG-pEDV-AVR-Pii-mCN and subsequently incubated at 27°C. Confocal microscopy was performed, on the third day of imbibition, after washing the leaf disks with distilled water and without peeling the epidermis. For *N. benthamiana* experiments, bacterial inocula (OD₆₀₀ = 0.45) were infiltrated to leaves of 18-day-old plants using a 1 ml-syringe without a needle. Eighteen hours after infection, *N. benthamiana* leaves were injected with DAPI staining solution (1 µg ml⁻¹ in 0.1% DMSO) to confirm the nuclear signal. Confocal microscopy was performed after 5 min of DAPI treatment. The DAPI fluorescence was analyzed with an Olympus BX61 fluorescence microscope (Olympus, <http://www.olympus.com/>) with a filter set of U-MWU2 (excitation filter 330–385 nm; emission filter 420 nm). Healthy or BG-pEDV inoculated leaves or leaf sheaths were used as controls and for checking autofluorescence. mCherry fluorescence was observed using an Olympus FluoView FV1000-D confocal laser-scanning microscope (configuration with BX61, Olympus) equipped with a Multiargon laser, a HeNe G laser, a 40xUPlanSApo (0.9 numerical aperture) and a 60xUPlanFLN (0.9 numerical aperture) objective lens. Samples were mounted in water under cover slips and excited with the He/Ne laser. We used a DM488/543/633 dichroic mirror, a SDM630 beam splitter and a BA560-600 emission filter.

Immunoprecipitation and detection of AVR:mCherry:NLS fusion proteins in planta

Leaves of 3-week-old *N. benthamiana* plants were infiltrated with BG-pEDV-AVR-Pik-mCN or BG-pEDV-AVR-Pii-mCN of OD₆₀₀ = 2.0 using a 1-ml syringe without a needle. Leaf samples taken 10 HPI were ground in liquid nitrogen and solubilized in extraction buffer containing 10 mM DTT, 2% polyvinylpyrrolidone and protease inhibitor cocktail. The extracts were immunoprecipitated using anti HA- (Sigma) or anti RFP- (MBL, <http://www.mblintl.com/>) conjugated agarose beads as described by Win *et al.* (2011). The precipitated proteins were labeled using anti-HA-HRP antibody (Roche), and detected using an ECL-advance detection kit.

ACKNOWLEDGEMENTS

This work was supported by the 'Program for Promotion of Basic Research Activities for Innovative Biosciences (PROBRAIN)' (Japan) and Japan Society for the Promotion of Science (JSPS) grants no. 18310136 and 20380027, and 'The Ministry of Agriculture, Forestry, and Fisheries of Japan (Genomics for Agricultural Innovation PMI-0010)' and the Ministry of Education, Culture,

Sports, Science and Technology of Japan (Grant-in-Aid for Scientific Research on Innovative Areas 23113009); and by JSPS grant nos 22780040 and 2301518 to H. Saitoh, JSPS grant no. 2200214 to R. Terauchi. The financial assistance received from JSPS to Shailendra Sharma and Shiveta Sharma for carrying out this study is gratefully acknowledged. S. Kamoun and J.D.G. Jones were supported by The Gatsby Foundation (United Kingdom).

SUPPORTING INFORMATION

Additional Supporting Information may be found in the online version of this article.

Figure S1. mCherry fusion proteins of AVR-Pik and AVR-Pii retain their Avr function.

Figure S2. Confocal laser-scanning microscopy analysis (confocal microscopy) of non-inoculated and BG-pEDV-inoculated rice leaf sheaths did not show any red fluorescence in nuclei of the cells.

Figure S3. N-terminal HA fusions of AVR-Pik and AVR-Pii retain their Avr function.

Table S1. Primers used for RT-PCR.

REFERENCES

- Boller, T. and He, S.Y. (2009) Innate immunity in plants: an arms race between pattern recognition receptors in plants and effectors in microbial pathogens. *Science*, **324**, 742–744.
- Bozkurt, T.O., Schornack, S., Banfield, M.J. and Kamoun, S. (2012) Oomycetes, effectors, and all that jazz. *Curr. Opin. Plant Biol.* **15**, 1–10.
- Casper-Lindley, C., Dahlbeck, D., Clark, E.T. and Staskawicz, B.J. (2002) Direct biochemical evidence for type III secretion-dependent translocation of the AvrBs2 effector protein into plant cells. *Proc. Natl Acad. Sci. USA*, **99**, 8336–8341.
- Couch, B.C. and Kohn, L.M. (2002) A multilocus gene genealogy concordant with host preference indicates segregation of a new species, *Magnaporthe oryzae*, from *M. grisea*. *Mycologia*, **94**, 683–693.
- Debroy, S., Thilmony, R., Kwack, Y.-B., Nomura, K. and He, S.Y. (2004) A family of conserved bacterial effectors inhibits salicylic acid-mediated basal immunity and promotes disease necrosis in plants. *Proc. Natl Acad. Sci. USA*, **101**, 9927–9932.
- Fabro, G., Steinbrenner, J., Coates, M. *et al.* (2011) Multiple candidate effectors from the oomycete pathogen *Hyaloperonospora arabidopsidis* suppress host plant immunity. *PLoS Pathog.* **7**, e1002348.
- Ham, J.Y., Melanson, R.A. and Rush, M.C. (2011) *Burkholderia glumae*: next major pathogen of rice? *Mol. Plant Pathol.* **12**, 329–339.
- Hann, D.R., Gimenez-Ibanez, S. and Rathjen, J.P. (2010) Bacterial virulence effectors and their activities. *Curr. Opin. Plant Biol.* **13**, 388–393.
- van der Hoorn, R.A. and Kamoun, S. (2008) From Gurad to Decoy: a new model for perception of plant pathogen effectors. *Plant Cell*, **20**, 2009–2017.
- Jeong, Y., Kim, J., Kim, S. and Kang, Y. (2003) Toxoflavin produced by *Burkholderia glumae* causing rice grain rot is responsible for inducing bacterial wilt in many field crops. *Plant Dis.* **87**, 890–895.
- Jones, J.D.G. and Dangl, J.L. (2006) The plant immune system. *Nature*, **444**, 323–329.
- Kamoun, S. (2006) A catalogue of the effector secretome of plant pathogenic oomycetes. *Annu. Rev. Phytopathol.* **44**, 41–60.
- Kang, Y., Kim, J., Kim, S., Kim, H., Lim, J.Y., Kim, M., Kwak, J., Moon, J.S. and Hwang, I. (2008) Proteomic analysis of the proteins regulated by HrpB from the plant pathogenic bacterium *Burkholderia glumae*. *Proteomics*, **8**, 106–121.
- Khang, C.H., Berruyer, R., Giraldo, M.C., Kankanala, P., Park, S.-Y., Czymbek, K., Kang, S. and Valent, B. (2010) Translocation of *Magnaporthe oryzae* effectors into rice cells and their subsequent cell-to-cell movement. *Plant Cell*, **22**, 1388–1403.
- Kim, J., Kang, Y., Kim, J.G., Choi, O. and Hwang, I. (2010) Occurrence of *Burkholderia glumae* on rice and field crops in Korea. *Plant Pathol. J.* **26**, 271–272.
- Koeck, M., Hardham, A.R. and Dodds, P.N. (2011) The role of effectors of biotrophic and hemibiotrophic fungi in infection. *Cell. Microbiol.* **13**, 1849–1857.

- Kosugi, S., Hasebe, M., Tomita, M. and Yanagawa, H. (2008) Nuclear export signal defined using a localization-based yeast selection system. *Traffic*, **8**, 2053–2062.
- Mosquera, G., Giraldo, M.C., Khang, C.H., Coughlan, S. and Valent, B. (2009) Interaction transcriptome analysis identifies *Magnaporthe oryzae* BAS1-4 as biotrophy-associated secreted proteins in rice blast disease. *Plant Cell*, **21**, 1273–1290.
- Mueller, O., Kahmann, R., Aguilar, G., Trejo-Aguilar, B., Wu, A. and de Vries, R.P. (2008) The secretome of the maize pathogen *Ustilago maydis*. *Fungal Genet. Biol.* **45**, S63–S70.
- Nandakumar, R., Shahjahan, A.K.M., Yuan, X.L., Dickstein, E.R., Groth, D.E., Clark, C.A., Cartwright, R.D. and Rush, M.C. (2009) *Burkholderia glumae* and *B. gladioli* cause bacterial panicle blight in rice in the southern united states. *Plant Dis.*, **93**, 896–905.
- Rentel, M.C., Leonelli, L., Dahlbeck, D., Zao, B. and Staskawics, B.J. (2008) Recognition of the *Hyaloperonospora parasitica* effector ATR13 triggers resistance against oomycete, bacterial, and viral pathogens. *Proc. Natl Acad. Sci. USA*, **105**, 1091–1096.
- Saitoh, H., Fujisawa, S., Mitsuoka, C. *et al.* (2012) Large-scale gene disruption in *Magnaporthe oryzae* identifies MC69, a secreted protein required for infection by monocot and dicot fungal pathogens. *PLoS Pathog.* **8**, e1002711.
- Schechter, L.M., Roberts, K.A., Jamir, Y., Alfano, J.R. and Collmer, A. (2004) *Pseudomonas syringae* type III secretion system targeting signals and novel effectors studied with a Cya translocation reporter. *J. Bacteriol.* **186**, 543–555.
- Sohn, K.H., Lei, R., Nemri, A. and Jones, J.D.G. (2007) The downy mildew effector proteins ATR1 and ATR13 promote disease susceptibility in *Arabidopsis thaliana*. *Plant Cell*, **19**, 4077–4090.
- Stassen, J.H.M. and Van den Ackerveken, G. (2011) How do oomycete effectors interfere with plant life? *Curr. Opin. Plant Biol.* **14**, 407–414.
- Takano, Y., Komeda, K., Kojima, K. and Okuno, T. (2001) Proper regulation of cyclic AMP-dependent protein kinase is required for growth, conidiation, and appressorium function in the anthracnose fungus *Colletotrichum lagenarium*. *Mol. Plant-Microbe Interact.* **14**, 1149–1157.
- Talbot, N.J. (2003) On the trail of a cereal killer. *Annu. Rev. Microbiol.* **57**, 177–202.
- Thomma, B.P.H.J., Nürnberger, T. and Joosten, M.H.A.J. (2011) Of PAMPs and effectors: the blurred PTI-ETI dichotomy. *Plant Cell*, **23**, 4–15.
- Tomita, R., Sekine, K.-T., Mizumoto, H., Sakamoto, M., Murai, J., Kiba, A., Hikichi, Y., Suzuki, K. and Kobayashi, K. (2011) Genetic basis for the hierarchical interaction between *Tobamovirus* spp. and *L* resistance gene alleles from different pepper species. *Mol. Plant-Microbe Interact.* **24**, 108–117.
- Triplett, L.R., Melotto, M. and Sundin, W. (2009) Functional analysis of the N terminus of the *Erwinia amylovora* secreted effector DspA/E reveals features required for secretion, translocation, and binding to the chaperone DspB/F. *Mol. Plant-Microbe Interact.* **22**, 1282–1292.
- Tsushima, S., Naito, H. and Koitabashi, M. (1996) Population dynamics of *Pseudomonas glumae*, the causal agent of bacterial grain rot of rice, on leaf sheaths of rice plants in relation to disease development in the field. *Ann. Phytopathol. Soc. Jpn.* **62**, 108–113.
- Valent, B. (1990) Rice blast as a model system for plant pathology. *Phytopathology*, **80**, 33–36.
- Whisson, S.C., Boevink, P.C., Moleleki, L. *et al.* (2007) A translocation signal for delivery of oomycete effector proteins into host plant cells. *Nature*, **450**, 115–118.
- Win, J., Kamoun, S. and Jones, A.M.E. (2011) Purification of effector-target complexes via transient expression in *Nicotiana benthamiana*. *Methods Mol. Biol.* **712**, 181–193.
- Yoshida, K., Saitoh, H., Fujisawa, S. *et al.* (2009) Association genetics reveals three novel avirulence genes from the rice blast fungal pathogen *Magnaporthe oryzae*. *Plant Cell*, **21**, 1573–1591.
- Zeigler, R.S., Tohme, J., Nelson, R.J., Levy, M. and Correa, F.J. (1994) Lineage exclusion: a proposal for linking blast population analysis to resistance breeding. In *Rice Blast Disease* (Zeigler, R.S., Leong, S.A. and Teng, P.S., eds). Los Banos, Laguna, Philippines: CAB International; International Rice Research Institute (IRRI), pp. 267–292.
- Zipfel, C. (2009) Early molecular events in PAMP-triggered immunity. *Curr. Opin. Plant Biol.* **12**, 414–420.